

# Solid-state transformations during diffusion bonding of copper to iron

F. A. CALVO, A. UREÑA, J. Ma. GOMEZ de SALAZAR, F. MOLLEDA, A. J. CRIADO

*Department of Materials Science and Metallurgical Engineering, Faculty of Chemical Science, University of Madrid, Spain*

Solid-state bonding between dissimilar metals, produced at elevated temperatures with the application of a bonding pressure, causes structural changes in the microstructure of the zones nearest to the bond interface. These metallurgical transformations, produced by interdiffusion in the vicinity of the bond, decide the final properties of the joint. In the present paper, such diffusional transformations have been investigated for diffusion-bonded joints of Armco iron and copper with different oxygen contents (ETPC and OFLPC). The formation of iron oxide (wustite) has been observed in the ETPC-Armco iron joints. This oxide did not appear in OFLPC-Armco iron diffusion-bonded joints. This suggests that iron oxide forms by reaction of iron with oxygen dissolved in the ETPC base metal. The formation of copper particles in the iron base matrix, near the bond interface, has been observed. This may be due to two different processes: the solid-state precipitation of copper into iron and the eutectoid reaction ( $\gamma \rightarrow \varepsilon + \alpha$ ) at bonding temperatures above 900°C.

## 1. Introduction

Diffusion bonding is a suitable method for joining a dissimilar-metal combination [1-4]. The metals are joined by causing the coalescence of the metallic surfaces, by the application of pressure at elevated temperature for a finite interval. This technique produces joints with a minimum macroscopic deformation and without deterioration in the mechanical properties of the base metals, because the bonding is carried out below the solidus temperature (about  $0.7T_m$  for the lowest melting-point metal) under a suitable pressure [5-7].

However, in the diffusion bonding of dissimilar metals, microstructural changes are produced in the base metals adjacent to the bond interface, and the final mechanical properties of the bond will be determined by the microstructure of this interface region. In the present work, such structural changes have been investigated for the diffusion bonding between iron and copper. This is a typical example of bonding between two metals with a low inter-solubility, that are immiscible phases in the solid state.

The influence of the oxygen level in the base copper has also been investigated.

## 2. Experimental procedures

### 2.1. Equipment

The apparatus was designed to provide a compressive loading and heating of the bond zone between iron and copper, in a protective vacuum environment.

All bonds were made in a vacuum furnace with a radiant-resistance heater of tungsten wire. The bonding pressure was applied with a mechanical system (lever) with a lever arm ratio of 4.5:1 (Fig. 1).

The bonding temperature was measured by spot-welding a chromel-alumel thermocouple to the vicinity of the bond interface.

### 2.2. Materials and samples preparation

Base metals used in the present work were electrolytic tough pitch copper (ETPC), oxygen-free low phosphorus copper (OFLPC) and Armco iron, whose chemical compositions are shown in Table I. The base metals were machined cylinders, 15 mm diameter and 10 mm long.

The faying surface of the base metal was finished by grinding on emery paper of 1200 grade, and washing in an ultrasonic bath with acetone just before bonding. This produces adequate surface roughness but removes

TABLE I Chemical compositions of the base metals of electrolytic tough pitch copper (ETPC), oxygen-free low phosphorus copper (OFLPC) and Armco iron

Material	Composition (wt %)												
	Pb	C	Ni	Zn	P	S	N	O	P	Si	Cu	Mn	Fe
ETPC	0.004		0.005			0.002		0.04	—		Balance		0.007
OFLPC	0.002			0.004		—		—	0.005		Balance		0.004
Armco iron		0.004			0.004	0.007	0.005			0.001		0.03	Balance

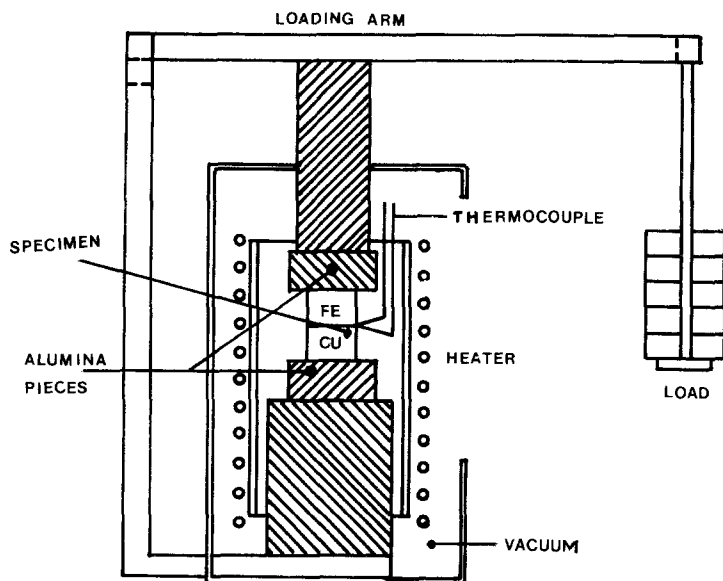


Figure 1 Diagram of the diffusion bonding unit.

contamination (oil, grease, dirt, etc.) and oxide film, which makes the contact between surfaces difficult and prevents the formation of a metallic bond between the faying surfaces [6].

### 2.3. Bonding procedure

Two types of diffusion-welded joints were made: ETPC to Armco iron and OFLPC to Armco iron. They were made in a vacuum environment of approximately  $10^{-4}$  to  $10^{-5}$  Pa. The bonding conditions used in all trials were: pressure ( $P_b$ ) between 1.15 and 3.85 MPa, temperature ( $T_b$ ) between 850 and 980°C and time ( $t_b$ ) varying from 0.2 to 40 h. The thermal bonding cycles are shown in Fig. 2.

The bonded samples were cut axially to the contact plane and this surface was prepared using conventional metallographic techniques. Due to the different nature of the two base metals, two chemical etches were used to reveal the microstructural changes in each diffusion zone. These etches were 2% Nital for Armco iron and  $\text{NH}_4\text{OH}$  (5 parts) +  $\text{H}_2\text{O}$  (5 parts) +  $\text{H}_2\text{O}_2$  (3%) (2 parts) for copper. The surface was examined by scanning electron microscopy (SEM).

## 3. Results and discussion

Metallographic study of the Cu–Fe joints indicated the existence of several diffusion zones near the bond interface. Different solid transformations had been

produced in these zones during the bonding, by diffusional phenomena.

Fig. 3 shows the microstructure of the two bonding zones of an ETPC–Armco joint after 2 h at 970°C. There is a narrow band in the ETPC base metal, adjacent to the bond interface, decorated by many dark-etching particles. The diffusion zone in the Armco iron is narrower than the ETPC zone, and it is characterized by preferential penetration into the iron grain boundaries. The characteristic microstructure of each zone will be studied in Sections 3.1. and 3.2.

### 3.1. Diffusion zone in the Armco iron

Different bonding trials were made for Armco iron–ETPC and Armco iron–OFLPC in order to determine the nature and development of this zone, under different bonding conditions. It was shown that the formation of this diffusion zone was not affected by the presence of oxygen in the base copper, however, its morphology and nature were variable with the temperature.

Joints produced at temperatures above 900°C had a very narrow diffusion layer parallel to the bond interface (Fig. 4). This layer was composed of a mixture of small quasispherical particles with diameter varying between 0.1 and 0.05  $\mu\text{m}$  (Fig. 5); energy-dispersive spectrometry (EDS) microanalysis proved that they were very rich in copper.

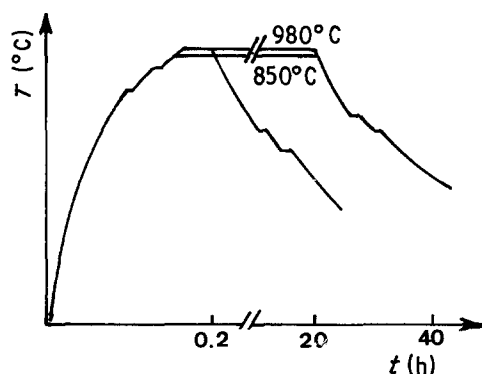


Figure 2 Thermal bonding cycles.

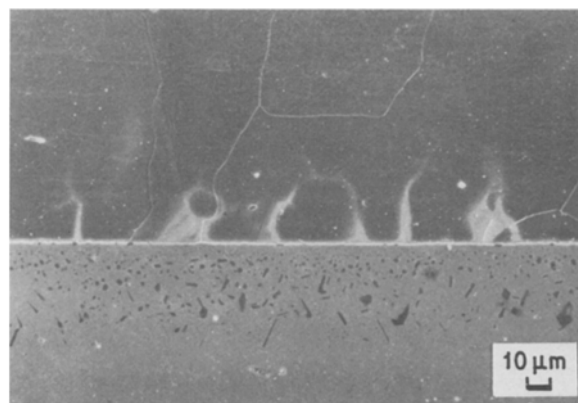


Figure 3 Scanning electron micrograph of bond of ETPC to Armco iron ( $t_b = 2$  h,  $T_b = 970^\circ\text{C}$ ,  $P_b = 385$  MPa).

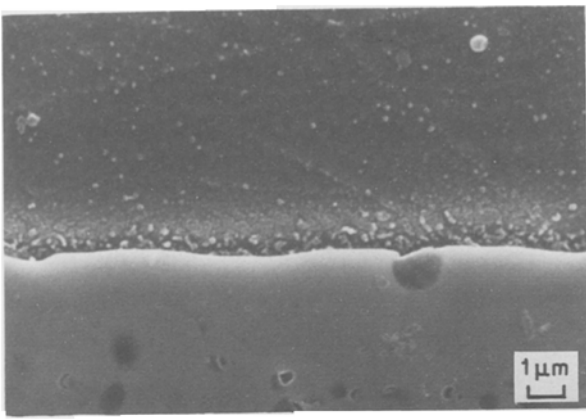


Figure 4 Eutectoid interlayer ( $\alpha + \epsilon$ ) in the base Armco iron of an ETPC–Armco iron joint after bonding for 2 h at 970° C.

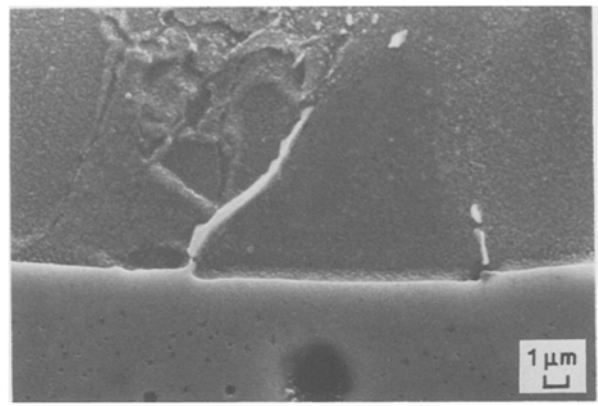


Figure 7 Pro-eutectoid  $\epsilon$  phase precipitated into grain boundary of Armco iron in ETPC–Armco iron joint ( $t_b = 6$  h,  $T_b = 970^\circ$  C,  $P_b = 2.5$  MPa).

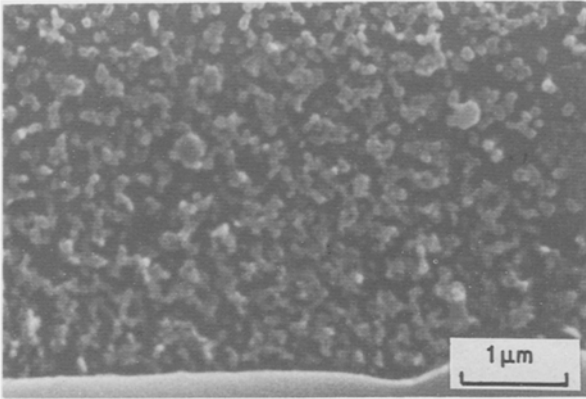


Figure 5 Detail of eutectoid layer.

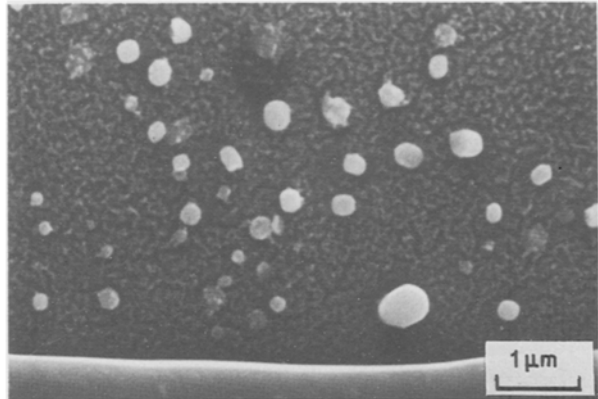


Figure 8  $\epsilon$  particles precipitated in iron. ETPC–Armco iron joint ( $t_b = 20$  h,  $t_b = 850^\circ$  C,  $P_b = 2.5$  MPa).

This diffusion layer penetrated the grain boundaries of the Armco iron, directly connected with interface (Fig. 6). After longer bonding times (more than 2 h), the morphology changed to elongated particles (Fig. 7).

Samples bonded at a temperature of 850° C presented a diffusion layer with different morphology. Again copper particles were present in the Armco iron matrix, but in this case these particles were less numerous (Fig. 8). After long bonding times (40 h) the particles became needle-like (Fig. 9).

The interpretation of these experimental results on the precipitation of copper into the Armco iron matrix may be explained by reference to the copper–iron equilibrium phase diagram (Fig. 10) [8]. The diffusion

of copper into  $\alpha$ -Fe produces a solid solution of limited solubility (2.4 wt % at 840° C) [9]. At temperatures above 910° C, the solid solution of copper in  $\gamma$ -Fe is stable. Cooling from the bonding temperature (950° C) induces the eutectoid transformation  $\gamma \rightleftharpoons \alpha + \epsilon$  at 835° C as follows from the Cu–Fe phase diagram [8]. The great difference in proportion of the two phases ( $\alpha/\epsilon = 49/1$ ) produces a divorced eutectoid. The copper-rich aggregates form the  $\epsilon$ -phase and the other eutectoid phase ( $\alpha$ ) is associated with the iron matrix.

Since the grain boundaries are high-diffusivity paths [10, 11], copper penetrates through them into the Armco iron matrix, far from the bond interface. When the bonding temperature is less than 900° C the diffusion of copper is more limited and its solubility in  $\alpha$ -Fe

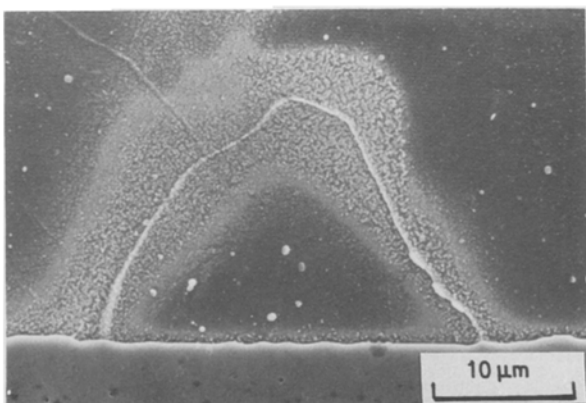


Figure 6 Penetration of the eutectoid layer into the grain boundaries of base iron.

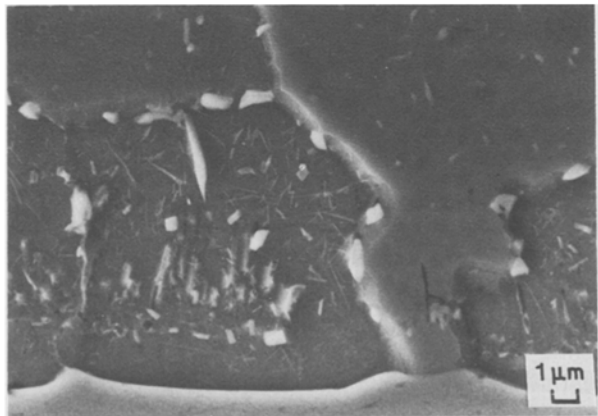


Figure 9 Rod-like growth of  $\epsilon$  phase precipitated in iron after bonding 40 h at 850° C.

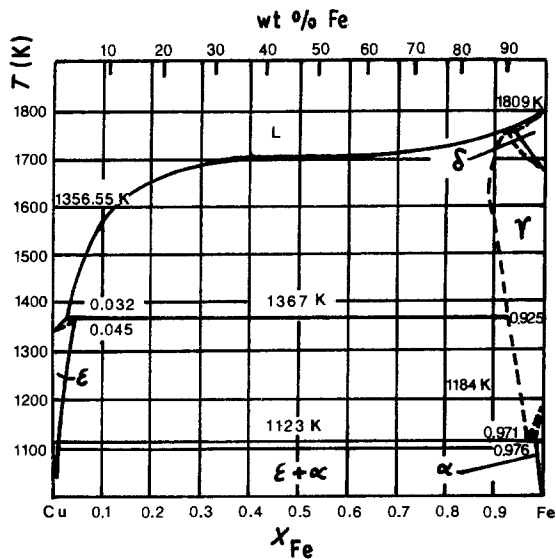


Figure 10 Iron-copper phase diagram [8].

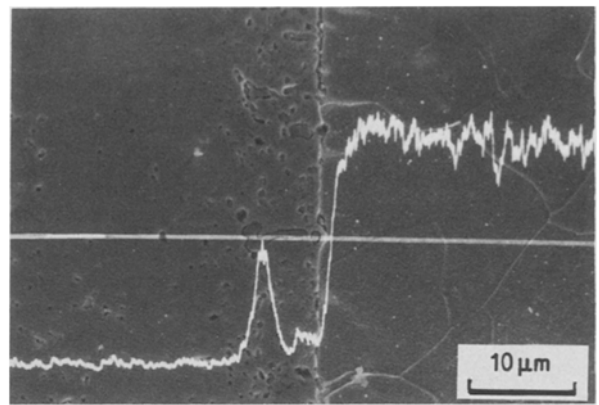


Figure 11 Scanning electron micrograph of the bond of ETPC to Armco iron ( $t_b = 15$  min,  $T_b = 950^\circ\text{C}$ ,  $P_b = 1.15$  MPa). The intensity of iron characteristic X-rays ( $K\alpha$ ) analysed along the white straight line is shown.

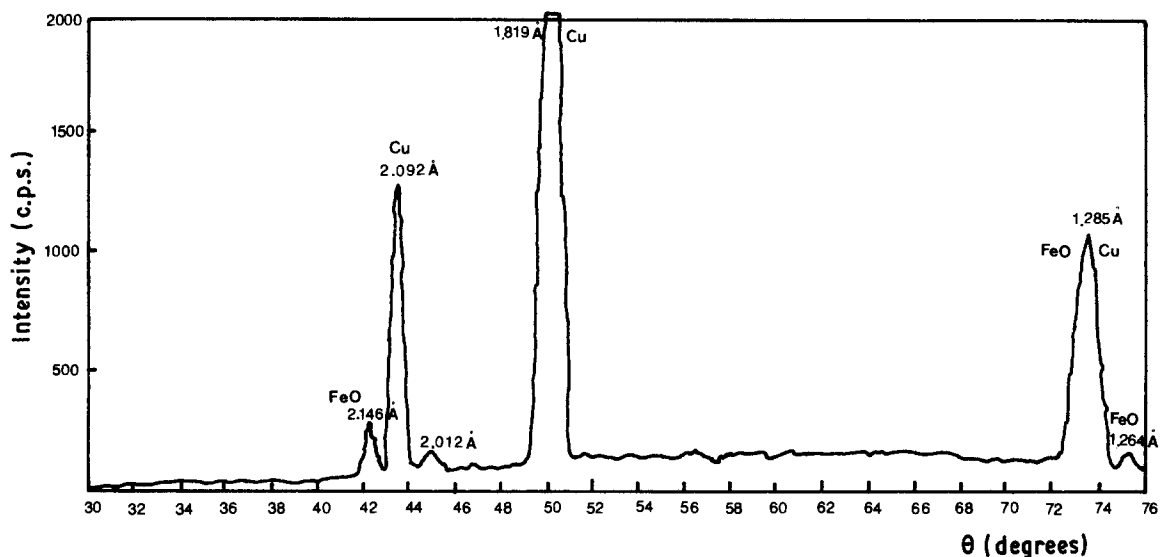


Figure 12 X-ray microdiffraction of the FeO precipitation layer in copper.  $1 \text{ \AA} = 0.1 \text{ nm}$ .

decreases with temperature. It produces a solid-state precipitation of copper in  $\alpha$ -iron. This phenomenon has been studied by other authors [12, 13]. They consider that copper precipitates from an iron as fcc  $\epsilon$ -phase without the formation of intermediate compounds.

Hornbogen and Glen [13] have proposed a three-stage mechanistic model for the precipitation of copper in  $\alpha$ -iron. In the first stage copper atoms form bcc spherical particles (clusters) coherent with the  $\alpha$ -Fe matrix and with diameters less than  $0.01 \mu\text{m}$ . These clusters are not pure copper, and at the beginning they have about 50 wt % of iron. During the second stage, the spherical particles change from bcc to fcc when they reach a critical size; this produces an incoherency with the matrix lattice. In the third stage, the spherical particles grow and rod-shaped particles are formed after longer times. This shape change is explained by Nabarro [14] as due to the decrease of the internal strain in the matrix caused by the presence of a precipitate.

### 3.2. Diffusion zone in the copper

The study of the diffusion zone of iron in copper was

based on the determination of the role played by oxygen present in the base copper during the bonding procedure.

Metallographic observation of the Armco-ETPC joints indicates the existence of a zone adjacent to the bond line with many particles of different morphologies

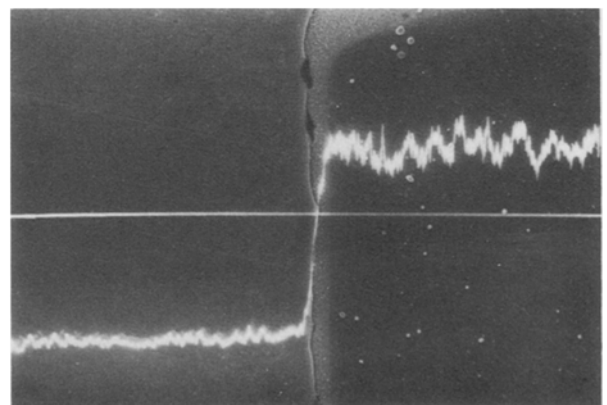


Figure 13 Scanning electron micrograph of the bond of OFLPC to Armco iron ( $t_b = 15$  min,  $T_b = 950^\circ\text{C}$ ,  $P_b = 1.15$  MPa). The intensity of iron characteristic X-rays ( $K\alpha$ ) analysed along the white straight line is shown.

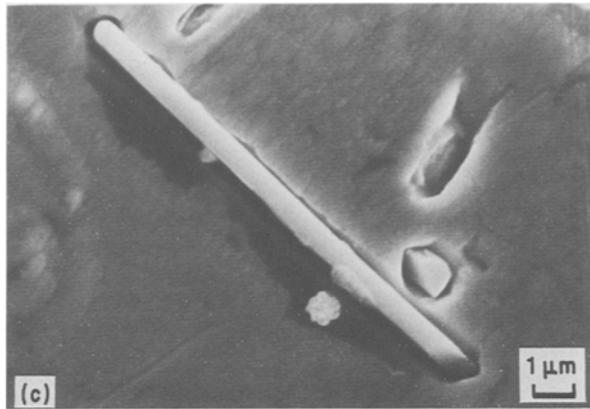
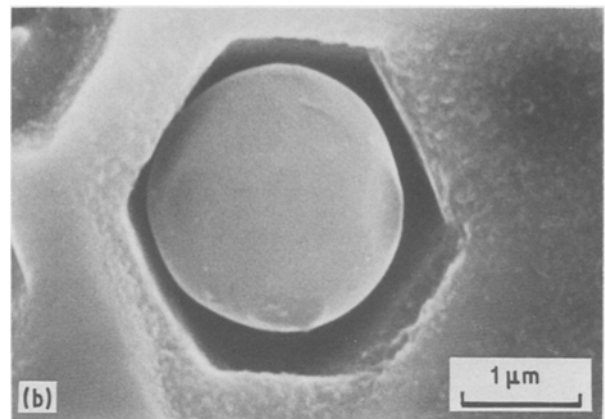
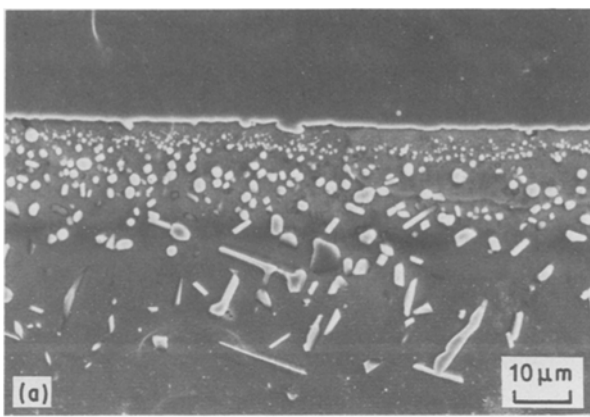


Figure 14 (a) Precipitation of FeO particles in ETPC. Joint bonded for 2 h at 970°C and 3.85 MPa. (b) Spherical particle of FeO. (c) Rod-like particle of FeO.

(Fig. 3). Microanalysis shows that these particles were iron-rich oxide compounds. In order to investigate the distribution of iron in the bonding zone, the intensity of  $FeK\alpha$  radiation was analysed along the white straight line in Fig. 11. The intensity increased when one of these particles was intercepted, indicating that the iron concentration was higher in the particles than in the copper matrix close to the bond interface. This oxide phase was identified by X-ray microdiffraction, using the reflection method, as wustite ( $FeO$ ) (Fig. 12).

Since the solubility of iron in copper decreases when the temperature decreases (Fig. 10) [8], the precipitation of iron will occur in copper during cooling after the bonding. Since iron has a higher affinity for oxygen than copper [15], iron oxide (wustite) will be formed in the joints of ETPC–Armco iron. This phenomenon is similar to the one produced during the diffusion bonding of nickel and oxidized copper, studied by other authors [16].

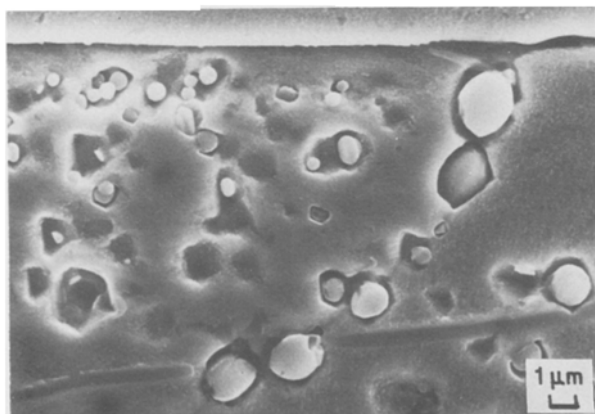


Figure 15 FeO particles precipitated in grain boundary of ETPC.

Several diffusion bonding trials between Armco iron and OFLPC were made to prove this fact. Fig. 13 shows one of these joints, without formation of FeO. This joint has been bonded under the same conditions as the iron–ETPC joint shown in Fig. 11.

Another interesting observation is the change in size and shape of the wustite particles with distance from the bond interface (Fig. 14a). In the nearest zone to the interface (Zone I) many spherical particles of diameter  $\approx 1 \mu m$  are formed (Fig. 14b). In an intermediate zone (Zone II) wustite particles grow but their number decreases. In the final zone large needles are formed when the bonding time is increased above 2 h (Fig. 14c).

The explanation of this phenomenon is based on the iron concentration gradient that exists in this narrow precipitation layer. This gradient favours FeO nucleation in the zone nearest to the interface (Zone I), while its growth is favoured in the last zone (Zone III).

It may be possible to explain the transition from spherical to needle shape during the growth of these particles. For particles of a size less than  $1 \mu m$ , surface energy may be the factor that determines the shape. When particles grow longer this factor becomes less important. Nabarro [14] showed that the strain energy of a non-coherent ellipsoidal particle will decrease in the following sequence: sphere  $\rightarrow$  needle  $\rightarrow$  disc, which could explain the needle shape of the FeO particles in the last zone of the bond interface.

It was also observed that FeO precipitation was favoured in the grain boundaries of the copper, in contact with the interface (Fig. 15). The precipitation of FeO limits the penetration of iron into base copper, but does not occur in the Armco iron–OFLPC joints and the penetration of iron is greater than in the Armco iron–ETPC, for the same bonding conditions (Fig. 16).

#### 4. Conclusions

1. The diffusion bonding between iron and copper produces several interdiffusion zones where different solid-state transformations are produced.
2. When Armco iron is bonded to copper above 900°C a eutectoid interlayer is formed in the base iron adjacent to the bond interface. This layer penetrates

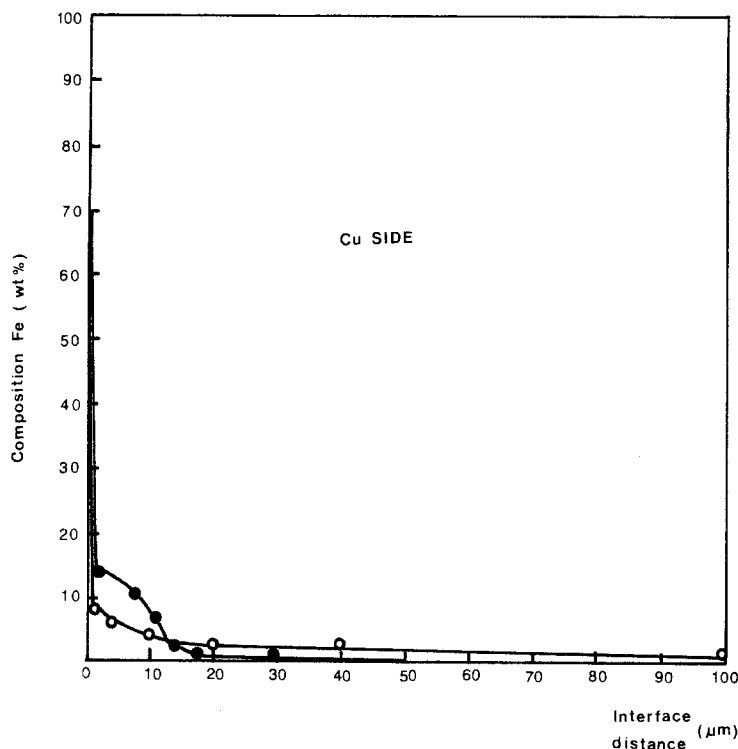


Figure 16 Concentration-penetration curve of iron through bond interface of (●) ETPC-Armco iron and (○) OFLPC-Armco iron joints for the same bonding conditions ( $t_b = 15$  min,  $T_b = 950^\circ\text{C}$ ,  $t_b = 1.15$  MPa).

into the grain boundaries of iron and its structure is a mixture of  $\epsilon$ -phase and base iron.

3. Joints bonded between  $800$  and  $900^\circ\text{C}$  show a narrow layer of precipitated copper ( $\epsilon$ -phase) formed in the base iron.

4. When ETPC is bonded to Armco iron, many particles of iron oxide (wustite) are observed in the ETPC adjacent to the bond interface. This phenomenon is not observed in OFLPC-Armco iron joints.

5. The formation of iron oxide is attributed to the reaction of iron with oxygen present in the ETPC. The diffusion penetration of iron into ETPC is limited by the precipitation of iron as FeO.

6. The size, shape and number of FeO precipitate particles change with the distance from the bond interface. These changes are attributed to the iron concentration gradient that exists in the diffusion zone.

## References

1. P. WEISNER, *Met. Constr. BWJ* **3** (1971) 91.
2. G. V. ALM, *Mater. Eng.* **70** (1969) 24.
3. J. KAWAKATSU and S. KITAYAMA, *Trans. JIM* **18** (1977) 455.
4. G. K. KHARCHENCO, T. V. SHEVCHUCK and A. I. IGNA TENKO, *Aut. Svarka* **10** (1978) 5.
5. W. A. OWZARSKI and D. F. PAULONIS, *Weld. J.* **60** (1981) 22.
6. P. M. BARTLE, *ibid.* **54** (1975) 799.
7. J. M. GERKEN and W. A. OWZARSKI, *Weld. Coun. Bull* **109** (1965) 1.
8. M. HANSEN, in "Constitution of Binary Alloys" (McGraw-Hill, London, 1958) p. 580.
9. H. A. WRIEDT and L. S. DARKEN, *AIME Trans.* **218** (1960) 30.
10. N. A. GJOSTEIN, in "Diffusion" (American Society for Metals, Metals Park, Ohio, 1973) p. 241.
11. G. MARTIN and B. PERAILLON, in "Grain Boundary Structure and Kinetics" (American Society for Metals, Metals Park, Ohio, 1980) p. 239.
12. S. R. GOODMAN, S. S. BRENNER and J. R. LOW, *Metall. Trans.* **4** (1973) 2363.
13. E. HORNOGEN and R. C. GLEN, *AIME Trans.* **218** (1960) 1064.
14. F. R. N. NABARRO, *Proc. R. Soc.* **A281** (1957) 1023.
15. F. D. RICHARDSON and J. H. E. JEFFES, *J. Iron Steel Inst.* **160** (1948) 261.
16. T. ENJO, K. IKEUCHI and N. AKIRAWA, *Trans. JWRI* **12** (1983) 59.

Received 10 February  
and accepted 18 June 1987